

## Original article



## Object-Based Image Analysis for Land Cover Mapping in an Urbanized Watershed

Tenaw G. Workie<sup>1</sup> and Tamene M. Hailu<sup>1</sup>

<sup>1</sup>College of Urban Development and Engineering, Ethiopian Civil Service University, Addis Ababa, Ethiopia

Received: 21 June 2021, Revised: 08 November 2021, Accepted: 02 December 2021

### ABSTRACT

Land cover maps are one of the thematic information sought among the remote sensing community and beyond for various applications. We intend to generate the land cover map of a watershed that encompasses Addis Ababa city to evaluate its contribution for flood hazard occurrence and quantification of flood risks. The study used Object Based Image Analysis (OBIA) to derive five land cover classes using Landsat 8 satellite images acquired in 25 March 2016. The satellite image was undergone to pre-processing, processing and post-processing steps involving radiometric and atmospheric corrections, fuzzy logic classification, and accuracy assessment. The accuracy assessment was made by comparing the reference data collected from Google earth and the classified image using various accuracy assessment measurements. The land cover map was generated with an overall accuracy of 94%, and with 92% Kappa Index of agreement (KIA). Land cover class specific accuracy measurements such as producers, users, Helden, short and KIA per class were also generated with values ranging between 79%-100%. The higher level of accuracy obtained is attributed to the image discontinuity and steeper gradients of the dominantly urbanized landscape which makes them easier to extract, and the robustness of the OBIA.

**Keywords:** Land cover; Object based image analysis; Accuracy assessment

### 1. Introduction

Remotely sensed data combined with developments in image analysis algorithms brought up opportunities to understand geographic phenomena over extensive areas fairly in a shorter period of time and with reasonable accuracies. Among the variety of products that are commonly generated from remotely sensed dataset includes land use/land cover. Land cover is taken as an indicator to the state of

the environment such as biodiversity and ecosystem health and used as an input for different environmental models. Attempts to produce land use/land cover with better accuracies have been one of the areas of research in the remote sensing community. The accuracy of the land cover produced from image classifications is dependent on the algorithms employed to generate the thematic layer among other factors as a result, developments of image processing



This work is licensed under a [Creative Commons Attribution-NonCommercial 4.0 International License](https://creativecommons.org/licenses/by-nc/4.0/).

algorithms are one of the research frontiers in the field of remote sensing. Image processing algorithms used to derive land cover can be broadly classified as pixel-based image analysis (PBIA) and object-based image analysis (OBIA). PBIA rely on basic image processing concepts developed in the 1970's which is based on image processing in a multi-dimensional feature space (Blaschke and Lang, 2006) but does not make use of a spatial concept (Blaschke and Strobl, 2001). Some of the limitation of pixel-based image analysis includes, pixels are not true geographic objects and pixel topologies are limited. Whereas, OBIA is a series of processing steps, in which the content analysis of the image (satellite or aerial) is applied to the recognition (segmentation), determination (classification), evaluation (accuracy and post-classification assessment) and analysis (e.g., changes, comparisons, mapping) of semantically clear spatial entities (homogeneous areas, structures, objects, phenomena) and not on the analysis of individual pixels (Veljanovski et al. 2011).

With increasing spatial resolution, pixel-based classification methods became less effective, since the relationship between the pixel size and the dimension of the observed objects on the Earth's surface has changed significantly. Therefore OBIA has become increasingly popular over the past decade and showed its advantage over PBIA. Several studies compared pixel- and object-based classification. They showed that satellite data of medium (e.g., Landsat TM/ETM+ and SPOT-5) and high resolution (Ikonos, QuickBird, WorldView) yields better results with the object-based approach (Baatz and Schäpe, 2000; Willhauck et al., 2000; Hay et al., 2005; Kamagata et al., 2005; Manakos et

al.2000; Whiteside and Ahmad, 2005; Yan et al. 2006). Moreover, numerous practical applications show that certain phenomena (presence of selected geographical objects) can be faster and more reliably detected with OBIA. On the other hand, studies showed that object-based classification did not outperform pixel-based classification on low-resolution satellite data (100 to 250 m) [3]. The drivers for a paradigm shift from PBIA to OBIA includes, a) demand for repeatable and transferable image analysis and feature extraction application of the growing high-resolution image availability, b) the ever growing and sophistication of use needs and expectations regarding geographic information products (Hay and Castilla, 2006) and c) developments of one commercial software called eCognition (Benz et al., 2004). Currently, other software packages integrate object-based modules such as ERDAS Imagine (module objective), ArcGIS (feature extraction) and ENVI (Feature extraction within ENVI Zoom). GeoMedia, RemoteView, SOCET SET, Genie Pro (Lavigne et al., 2006). The development of OBIA made spatial concepts in geography operational in image analysis. Spatial relations like distance, topological connectivity and directional characteristic, spatial patterns as well as multiple scales or regional construct are applied to objects based classification of image objects (Blaschke and Strobl, 2001). Next to the spectral characteristics of the resulting objects also other descriptive features are used such as shape information, boundary length, boundary length to specific other classes, neighborhood and distance relationship to other objects and classes to classify image objects (Blaschke and Lang, 2006). The

processes involved in OBIA are depicted in Figure 1.

Segments produced within the first step of object-based classification influence the final classification results (Blaschke et al., 2008). There is a causal relationship between segmentation and classification, as the particularities and errors of the first transfer onto the latter. Thus, the characteristics and quality of the attributes that are later used to evaluate

and sort objects are directly dependents on the way the segments are produced. This nature of the object-based approach can be illustrated by a spiral in which every step is based on the previous steps (Figure 2). The objective of the study was to map land cover of an urbanized watershed and the output of which is required for mapping flood hazard; a factor of flood risk in Addis Ababa City Administration along with other data.

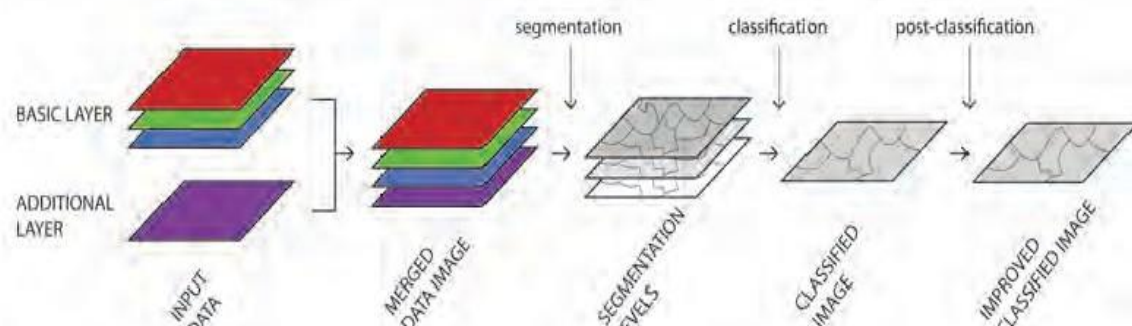


Figure 1: Processing steps in the object-based analysis of remote sensing data [3].

## 2. Materials and methods

### 2.1. Study Area

The study watershed lies between 453016.87 m and 494276.87 Easting and 969952.90 m and 1011572.90 m Northing (Figure 3). The area is about 106720.68 Ha. The watershed constitutes the capital city of Ethiopia: Addis Ababa, thus it

is a predominantly urbanized environment.

### 2.2 Data source

The land cover mapping is made from Landsat 8 image which is freely accessible from USGS website. It has 11 bands with a spatial resolution ranging from 15 to 100 (Table1).

$$L\lambda = ML \times Qcal + AL$$

1

Where,

$L\lambda$ =The Spectral Radiance at the sensor's aperture.,,  $L$ =Band-specific multiplicative rescaling factor from Landsat metadata (RADIANCE\_MULT\_BAND\_x, where x is the band number).

$AL$ =Band-specific additive rescaling factor from Landsat metadata (RADIANCE\_ADD\_BAND\_x, where x is the band number),  $Qcal$ =Quantized and calibrated standard product pixel values (DN).

### 2.2 Preprocessing

The Landsat 8 image acquired on 25 March 2016 underwent to preprocessing for radiometric and atmospheric corrections. The digital numbers (DN) were converted to spectral radiance at sensor followed by a FLAASH atmospheric correction to overcome atmospheric effects. The radiometric correction converts digital numbers (DN) of the image into spectral radiance using Equation 1. The radiance is then converted to surface reflectance by applying Fast Line-of-sight Atmospheric Analysis of Hypercubes (FLAASH). The preprocessed images are presented in Figure 4.

Table 1: Landsat 8 bands

Band #	μm	Resolution
1	0.433-0.453 (Aerosol)	30m
2	0.450-0.515 (Blue)	30m
3	0.525-0.600(Green)	30m
4	0.630-0.680(Red)	30m
5	0.845-0.885 (NIR)	30m
6	1.560-1.660 (SWIR1)	30m
7	2.100-2.300(SWIR2)	30m
8	0.500-0.680 (panchromatic)	30m
9	1.360-1.390 (cirrus)	30m
10	10.6-11.2 (TIRS1)	100m
11	11.5-12.5(TIRS 2)	100m

### 3. Object-Based Image Analysis (OBIA)

#### 3.1. Image segmentation

Image segmentation is vectorization of image objects. Object-based software embeds a variety of segmentation algorithms and most of them are categorized as the edge-based, the region growing, or a combination of the two (Schiewe, 2002). Which technique is better and more efficient, depends on the data (the character of the observed area), the selection of the parameters and the aim of the analysis (Nussbaum and Menz, 2008; Haralick and Shapiro, 1985). The preprocessed image was segmented using multi-resolution segmentation algorithm of eCognition software. All the image layers were weighted equally except the near infrared (NIR) which was weighted two times higher than the rest because of that fact that most of the land cover classes considered have distinguishable NIR signature.

The greatest challenge within object-based analysis is to perform satisfactory segmentation – achieve just the right number of spatial entities (objects) that differ in size and other characteristics – with a single procedure (Blaschke et al., 2008; Schiewe, 2002; Nussbaum and

Menz, 2008). We used Multi-resolution segmentation to generate image semantics. Multi-resolution segmentation starts at a pixel and the region of the image objects grow until constrained by a user defined rule set. After segmenting the image with different rule sets, the Scale parameter=25, Shape=0.2 and Compactness=0.8 are chosen as optimum parameters to segment the image into image objects (Figure 5). The scale parameter was determined by visual inspection of the resultant image objects after an iterative segmentation of the image with different scale parameters as the size of the image objects is highly sensitive to the scale parameter. The shape value is an indirect determination of to which percentage the spectral property defined the homogeneity criteria. The compactness criterion is used to optimize image objects with regard to compactness. This criterion should be used when different image objects which are rather compact, but are separated from non-compact objects only by a relatively weak spectral contrast. For the purpose that the land cover map was required, five land cover classes were defined. These include a) built-up, b) agriculture/bare land, c) dense woodland, d) Water body and e) grassland/sparse vegetation.

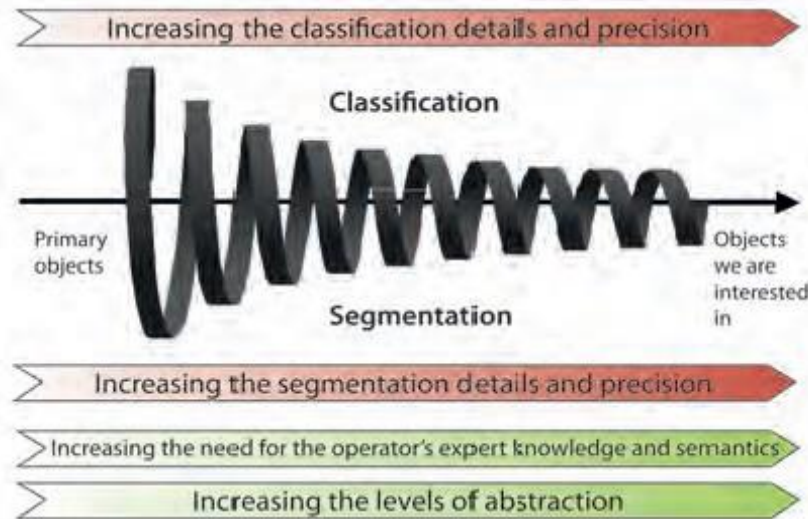


Figure 2: Common nature of the object-based classification process (Blaschke et al., 2008)

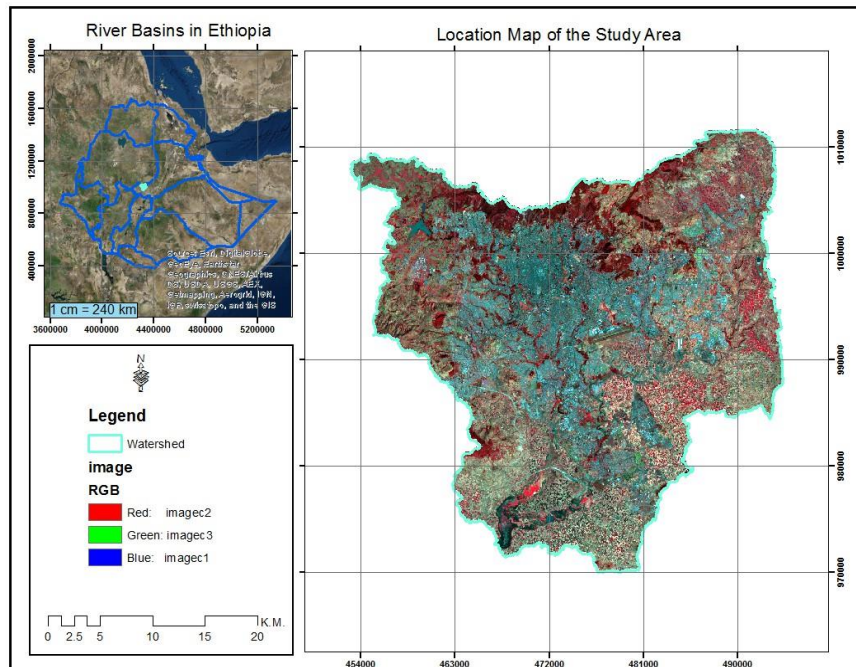


Figure 3: Map of the study area

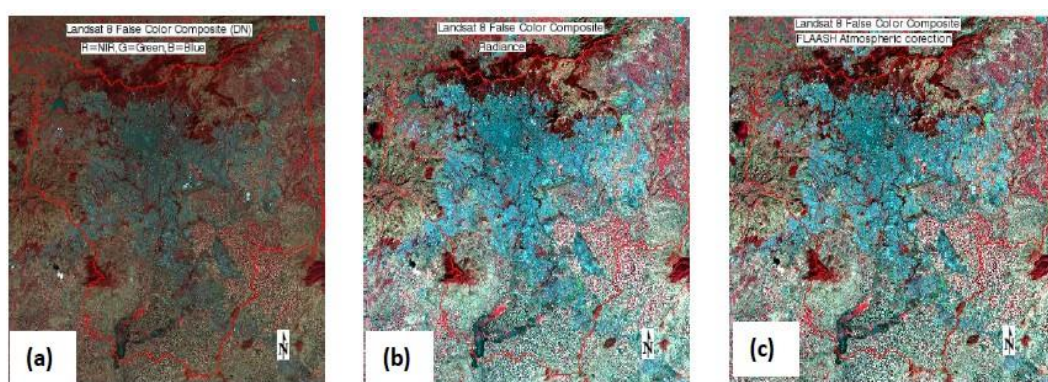


Figure 4: Raw image (DN values) (a), radiance (b) & atmospherically corrected reflectance (c)

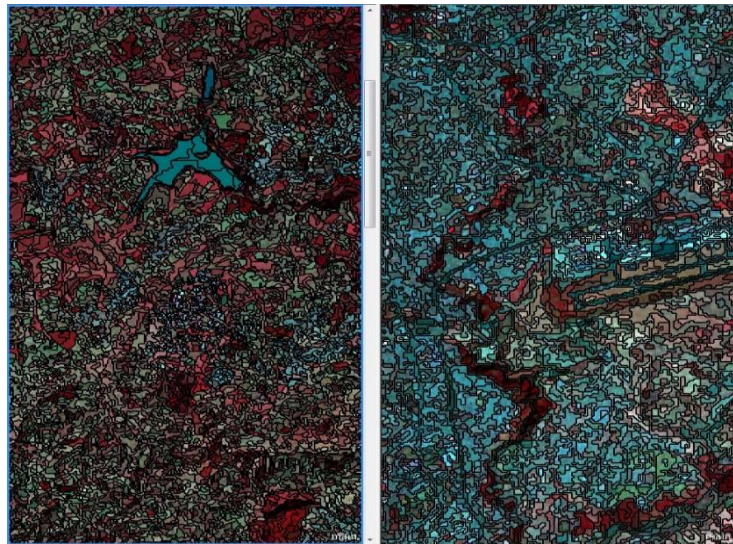


Figure 5: Image objects generated through Multi-resolution image segmentation algorithm.

### 3.2 Calculating indices and comparison for built-up cover extraction

Urban areas are a complex ecosystem constituting a myriad of heterogeneous materials (Akjol and Olaf, 2014). In heavily anthropogenic shaped landscapes discontinuities in an image are stronger and the gradients are steeper (Blaschke and Lang, 2006) and this makes distinguishing different land covers easier. A number of research works used different indices to effectively extract urban features particularly built-up areas. Three major image indices were derived and compared to each other using a membership function of training sites representing each land cover classes. Some studies, however, indicated that other land cover classes such as vegetation and water body are committed to built-up classes since they have positive NDBI values (Zha et al., 2003; Xu, 2007). To overcome this limitation (Xu 2008), developed IBI (Equation 3) which make use of three more indices namely, NDBI, Soil adjusted vegetation index (SAVI) and modification of normalized difference water index (MNDWI).

cover classes. These indices are the saturation index in the hue-saturation-intensity (HIS) color space, normalized built-up index (NDBI), and index-based built up index (IBI). In addition, normalized difference vegetation index (NDVI) was also calculated to support the extraction of land cover classes. Zha et al. (2003) developed NDBI which is based on the spectral response of built-up lands that have a higher reflectance in Middle infrared (MIR) band. This index takes the form of Equation 2 and NIR and SWIR2 bands of Landsat 8 were involved in calculating the index.

$$DBI = \frac{MIR-NIR}{MIR+NIR} \quad 2$$

$$IBI = \frac{NDBI - \frac{SAVI + MNDWI}{2}}{NDBI + \frac{SAVI + MNDWI}{2}} \quad 3$$

Where,

$$MNDWI = \frac{G-MIR}{G+MIR}$$

$$SAVI = \frac{NIR-R}{NIR+R+0.5}$$

MNDWI is supposed to enhance the contrast between the water body and the built-up area as the SAVI reduces the effect of the soil to create a contrast between the vegetation and the built-up area. Sazzad et al. (2013) also used

saturation index to extract built-up area with no overlap to other land cover classes than NDBI and IBI. The saturation index is expressed by Equation 4.

$$S = 1 - \frac{3}{(R+G+B)} \text{Min}(R, G, B) \quad 4$$

The effectiveness of the three indices (HIS saturation Index, NDBI and IBI) in effectively extracting built-up areas (Figure 6) were compared by the membership functions of the training data for all pairs of landcover (and found that HSI-Saturation index was resulting in minimum overlapping of built-up areas with other land covers (Table 2). Thus, in this study, the HSI-Saturation was used for classifying the built-up area. The HSI-saturation, however, resulted in commission error of other land cover classes such as water body and agricultural lands, thus the commission error was reduced partly by applying NDWI, NDBI, using fuzzy logic. Fuzzy logic, a knowledge-based method, widely used in pattern recognition today and is proposed to be applied in remote sensing image classification. Fuzzy logic makes no assumption about the statistical distribution of the data and it provides complete information for a thorough image analysis. It is interpretable and can use expert knowledge and training data at the same time. The major advantage of this theory is that it allows the natural description in linguistic terms of problems that should be solved rather than in terms of relationships between precise numerical values (Choodarathnakara et al., 2012). In a fuzzy representation for remote sensing image analysis, land-cover classes can be defined as fuzzy sets. A fuzzy set is a set of ordered pair which is given by  $A = \{x, \mu_A(x)\} : x \in X$ , where  $X$  is a universal set and  $\mu_A(x)$  is membership function the grade of the object  $x$  in  $A$  ( $0 \leq \mu_A(x) \leq 1$ ). For detail  $\mu_A(x)=0$  means that  $x$  does not belong to the  $A$ ,  $\mu_A(x)=1$  indicates that  $x$  fully belong to  $A$  and  $0 < \mu_A(x) < 1$  means that the  $x$  belong to the degree  $\mu_A$  (Thu et al., 2013).

and NDVI threshold values into the built-up class. NDVI was calculated using Equation 5.

$$NDVI = \frac{NIR-R}{NIR+R} \quad 5$$

### 3.3 Fuzzy logic classification

Image classification is the process of categorizing all the image objects/segments automatically into land cover classes (Choodarathnakara et a., 2012). Segment attributes describe the characteristics of individual segments and includes, geometric, spectral, textural, attributes of the spectrum band proportions (e.g., vegetation index), contextual (e.g., proximity of the neighboring pixels, distance), and temporal (e.g., time span, date, stability) (Navulur, 2007).

The segments generated in this study were classified based on segment attributes

The fuzzy logic system is an automatic system that is capable of mimicking human actions for a specific task. There are three main operations in a fuzzy logic system. The first operation is fuzzification, which is the mapping from a crisp point to a fuzzy set. The second operation is inferencing, which is the evaluation of the fuzzy rules in the form of IF-THEN. The last operation is defuzzification, which maps the fuzzy output of the expert system into a crisp value (Choodarathnakara et al., 2012; Navulur, 2007; Thu et al., 2013; Nedeljkovic, 2004).

In the fuzzification process, spectral indices relevant for extraction of the defined land cover classes were generated. This was followed by selecting appropriate indices for mapping each landcover classes with minimum overlap. For this purpose, comparison of the indices vis-à-vis paired land cover classes was conducted using membership functions of the training data (Table 2). Once the relevant index is identified, the threshold for defining each land cover classes was determined and this constitutes the inference of the fuzzy logic system. Eventually, defuzzification was

made as crisp thematic information is assigned for image objects/segments based on their membership values.

### 3.4 Accuracy assessment

The classification is usually validated on the basis of sample ground points with a known location and thematic content, regardless of the data scale. For a valid accuracy assessment, the compared data has to be harmonized from all aspects (spatial, temporal). The difference in the scale of the various data sources can lower the assessment quality since this means that the level of generalization varies from source to source. Such quantitative assessments are used to assess the probability of correct classification and the general quality or reliability of the classification results. Since all processing steps that lead to the final result also influence the final quality, more and more attention is given to the assessment of the quality of segmentation and semantic classification (Veljanovski et al., 2011). For the purpose of accuracy assessment of the classified image, ground reference points were collected at the centre of each land cover classes from Google earth images (Figure 7).

## 4. Results and discussion

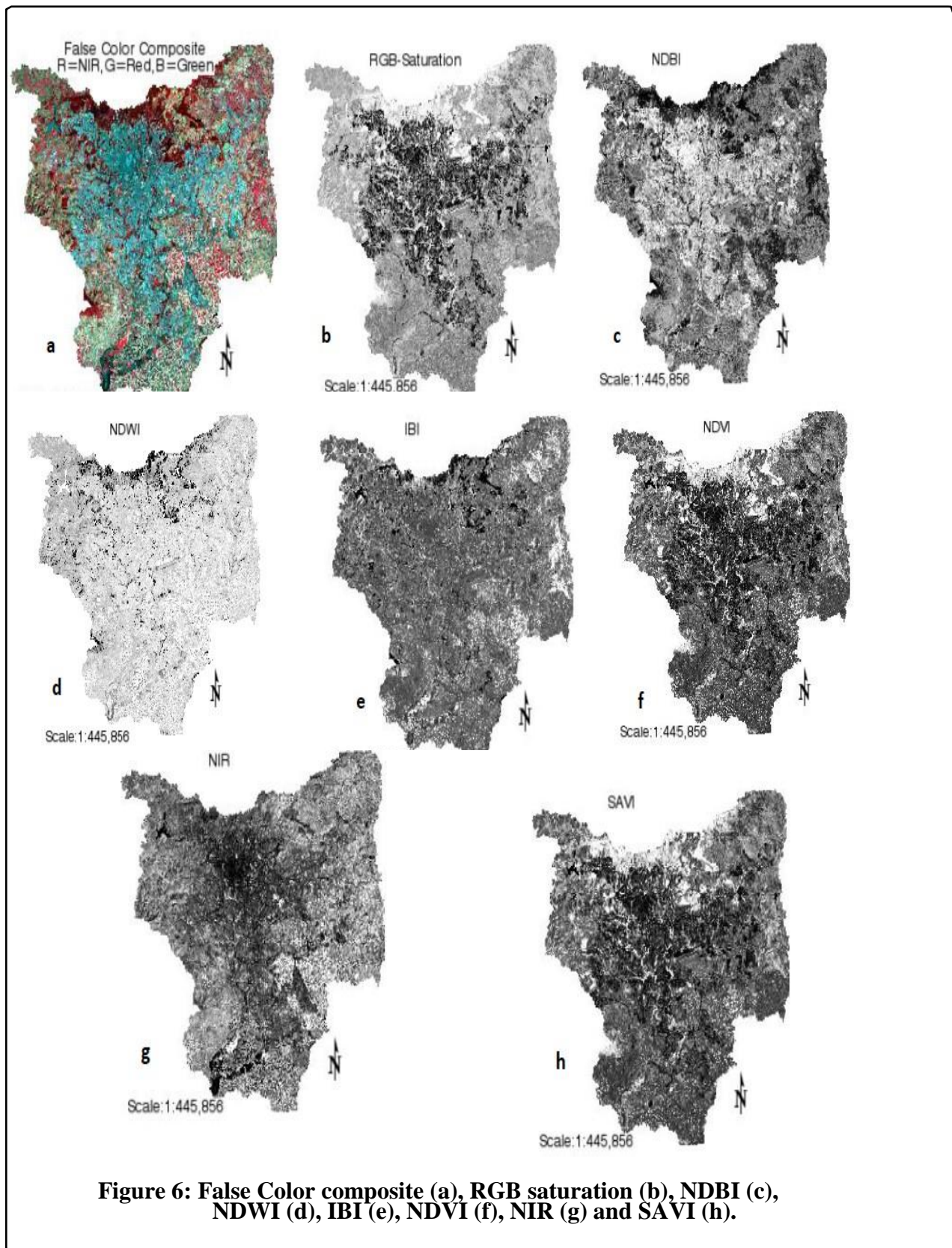
The landcover mapping is conducted with greater accuracy for the landcover types considered in this study (Table 3). The overall accuracy being about 94%, the accuracy levels for each specific land cover classes as measured using the accuracy indices presented in Table 3, varies slightly. The overall KIA also indicates very good agreement of the reference data and the classified map with a value of 92%. Dense woodland and water body are best classified compared to the other three land cover classes. All these measures only indicate the degree of agreement between the mapping results derived from analyzing the remote sensing data and those of the reference mapping [28]. Unaccounted uncertainties of the accuracy can be attributed to the biases

during sampling of the reference land covers; in terms of adequacy and representativeness, the mismatch between the segmented image objects and the actual land covers and the number of land cover classes mapped; as the explanatory power of all the accuracy measures are dependent on the number of classes (Hofmann and Lohmann, 2007).

The landcover mappings and land cover change detections conducted in Addis Ababa and the surrounding areas are pixel based and most of them didn't apply accuracy assessment of their classified images (Worako, 2016; Kassa et al., 2011) to compare this study with. However, given the areas is dominantly urban, spectral discontinuity in the image is abrupt and the gradients are steeper to readily and more accurately map landcover classes in such landscapes (Blaschke and Lang, 2006).

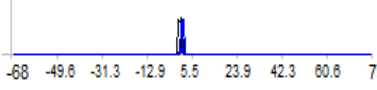
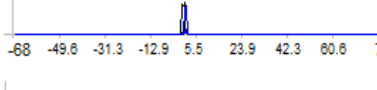
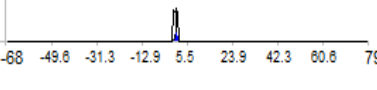
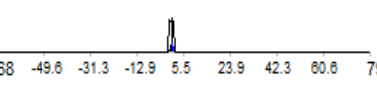
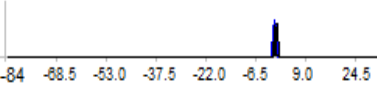
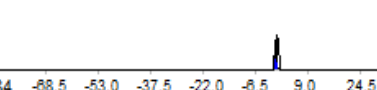
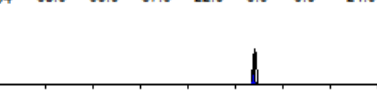
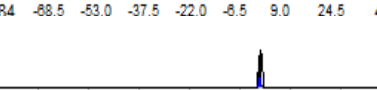
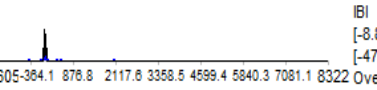
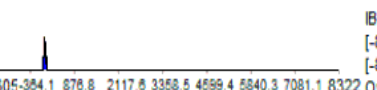
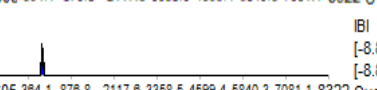
As can be observed in the landcover map in Figure 9, the woodlands areas are dominant in the northern parts of the watershed which represents the eucalyptus plantations at Entoto area. The Built- Up areas dominate the central part and the agriculture/bare land covers are surrounding the built-up or the periphery of the watershed. The only major water body is Gefersa water reservoir in the east and the water bodies around Aba-Samuel Lake in the south. The grassland/ sparse vegetations are found intermingling with woodland and agricultural lands.

The watershed constitutes Agriculture/bare land cover dominantly followed by built-up, and grassland/sparse vegetation accounting for about 41, 30, and 21% of the watershed, respectively. Only 8% of the area is dense woodland while the water bodies account less than 1% of the watershed. Table 4 shows the areas of each landcover classes.



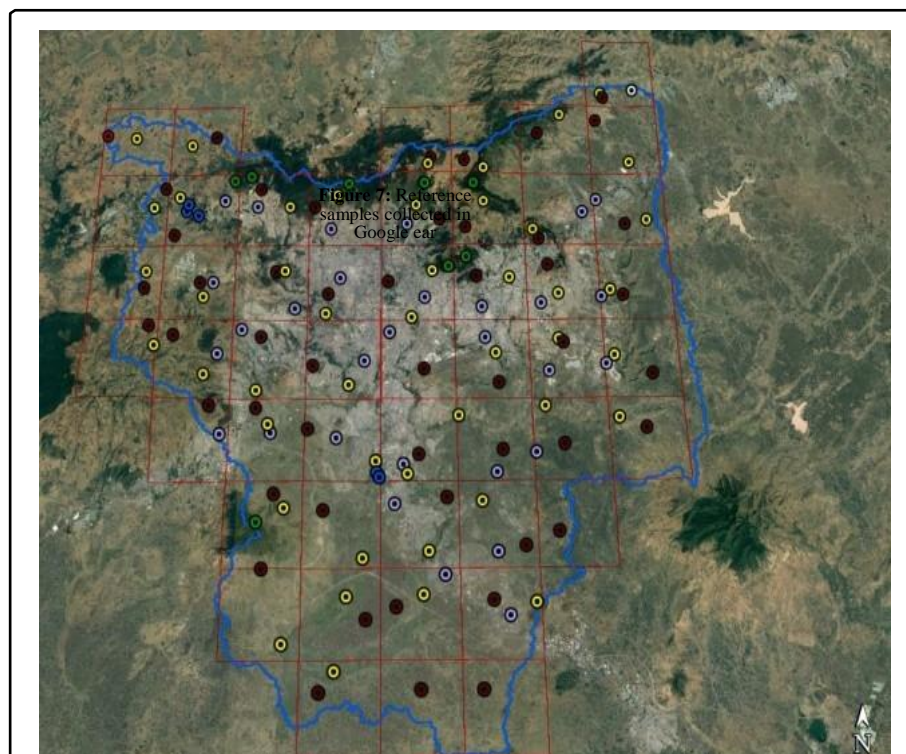
**Figure 6: False Color composite (a), RGB saturation (b), NDBI (c), NDWI (d), IBI (e), NDVI (f), NIR (g) and SAVI (h).**

**Table 2: Membership function of training samples of each land cover classes**

Land use type	HSI – Saturation Index (a)
Built-up Vs. Dense woodland	 <p>HSI Transformation Saturation(R=Infrared,G=Green,B=Blue) (NN) [-0.553 - 1.1764706] StdDev.: 0.1682971 [0.6 - 1.753] StdDev.: 0.04399944513 Overlap : 0.18</p>
Built-up Vs Grass/cropland	 <p>HSI Transformation Saturation(R=Infrared,G=Green,B=Blue) (NN) [-0.553 - 1.1764706] StdDev.: 0.1682971 [0.6 - 1.1764706] StdDev.: 0.02717181852 Overlap : 0.12</p>
Built-up Vs Water-body	 <p>HSI Transformation Saturation(R=Infrared,G=Green,B=Blue) (NN) [-0.553 - 1.1764706] StdDev.: 0.1682971 [0.02352941176 - 1.1764706] StdDev.: 0.1863375 Overlap : 0.27</p>
Built-up Vs Bare land	 <p>HSI Transformation Saturation(R=Infrared,G=Green,B=Blue) (NN) [-0.553 - 1.1764706] StdDev.: 0.1682971 [0.6 - 1.1764706] StdDev.: 0.04527850455 Overlap : 0.29</p>
<b>NDBI (b)</b>	
Built-up Vs Dense woodland	 <p>NDBI (NN) [-0.847 - 0.1254902] StdDev.: 0.1254822 [-1.3333333 - -0.3607843] StdDev.: 0.03570124157 Overlap : 0.38</p>
Built-up Vs Grass/cropland	 <p>NDBI (NN) [-0.847 - 0.1254902] StdDev.: 0.1254822 [-0.847 - -0.3607843] StdDev.: 0.06135185187 Overlap : 0.34</p>
Built-up Vs Water-body	 <p>NDBI (NN) [-0.847 - 0.1254902] StdDev.: 0.1254822 [-1.3333333 - -0.3607843] StdDev.: 0.03597076488 Overlap : 0.18</p>
Built-up Vs Bare land	 <p>NDBI (NN) [-0.847 - 0.1254902] StdDev.: 0.1254822 [-1.3333333 - -0.3607843] StdDev.: 0.172 Overlap : 0.34</p>
<b>IBI (c)</b>	
Built-up Vs Dense woodland	 <p>IBI [-8.8941176 - 30.0352941] StdDev.: 1.4334558 [-8.8941176 - 30.0352941] StdDev.: 3.3513240 Overlap : 0.85</p>
Built-up Vs Grass/cropland	 <p>IBI [-8.8941176 - 30.0352941] StdDev.: 1.4334558 [-476.047 - 2054.3647059] StdDev.: 196.4573428 Overlap : 0.18</p>
Built-up Vs Water-body	 <p>IBI [-8.8941176 - 30.0352941] StdDev.: 1.4334558 [-8.8941176 - 30.0352941] StdDev.: 1.2293526 Overlap : 0.36</p>
Built-up Vs Bare land	 <p>IBI [-8.8941176 - 30.0352941] StdDev.: 1.4334558 [-8.8941176 - 30.0352941] StdDev.: 0.5754998 Overlap : 0.34</p>

**Table 3: Confusion matrix of the accuracy assessment (Based on TTA Mask)**

User/ Reference	Built-up	Agriculture /bare land	Dense woodland	Water body	Grassland/ Sparse vegetation	Sum
Built-up	38	10	0	0	0	48
Agriculture/bare land		134	0	0	16	150
Dense Woodland		0	43	0	0	43
Water body		0	0	43	0	43
Grassland/ Sparse Vegetation		0	0	0	167	167
<b>Accuracy</b>						
Producer	1	0.93	1	1	0.91	
User	0.79	0.89	1	1	1	
Helden	0.88	0.91	1	1	0.95	
Short	0.79	0.84	1	1	0.91	
Kappa Index of Agreement (KIA) PER CLASS	1	0.83	1	1	0.91	
Overall KIA						0.94
						0.92



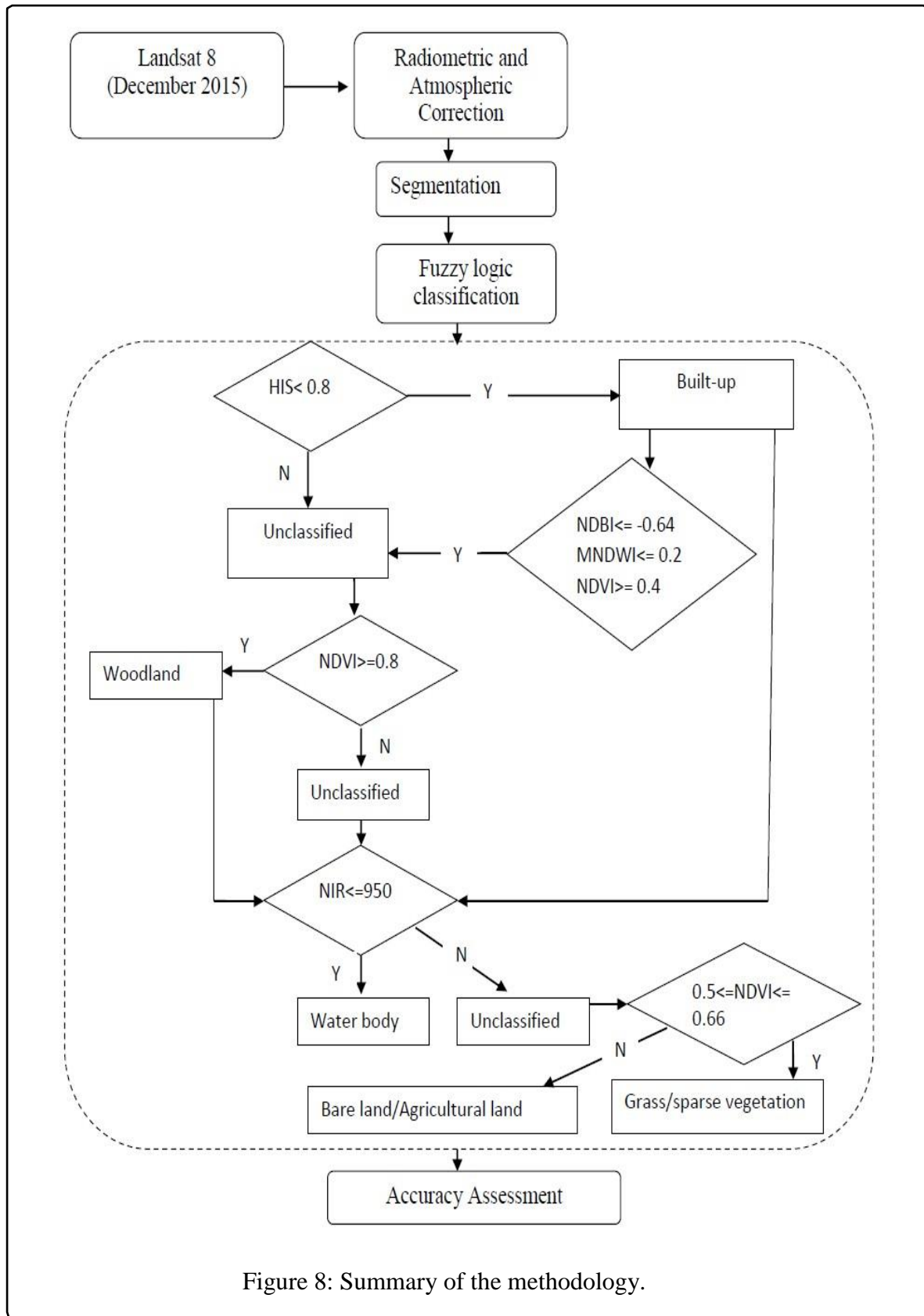


Figure 8: Summary of the methodology.

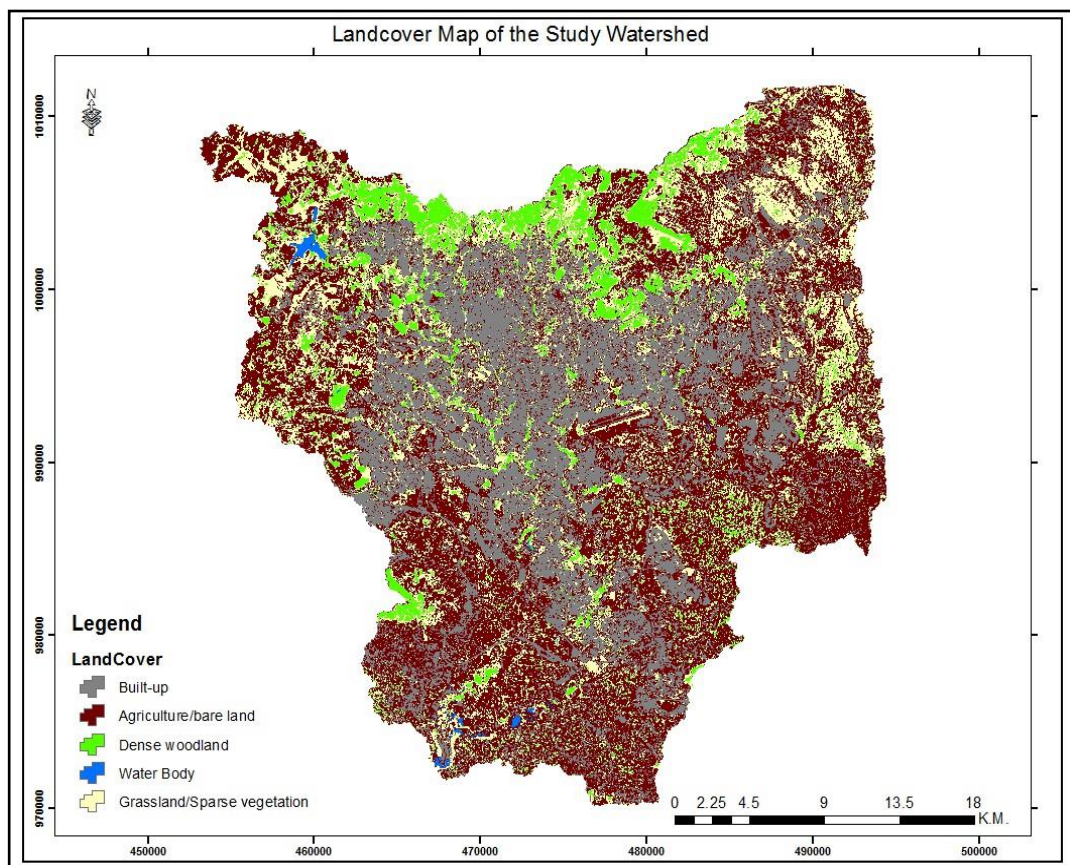


Figure 9: Land cover map of the study area.

Table 4: Statistics of land cover classes.

Landcover	Area(Hectare)	Area (%)
Built-up	30924	28.98
Agriculture/Bare land	43673.67	40.92
Dense woodland	9022.25	8.44
Grassland/sparse vegetation	22785.48	21.35
Water-body	327.96	0.31
Total	10,6722.36	100

## 5. Conclusion

OBIA of satellite images is a powerful approach for land cover mapping. Not only it creates more meaningful image objects through segmentation, but also helps to classify them based on their spectral, morphological, geometrical and spatial associations with other objects. In addition to the relative ease of mapping land cover types in urban dominated areas due to the heterogeneity of features and the resultant discontinuity and steeper

spectral gradients of the image, the OBIA is responsible for the higher levels of accuracy obtained in this study. However, it has to be noted that beyond what the accuracy measurements tell, the landcover map is embedded with uncertainties due to biases in a sampling of the reference data, determining the land cover types and the generalizations made during the process of segmentation of image objects. The Google-earth environment also found a useful platform with respect to collecting reference data for

accuracy assessment purpose. This has made accuracy assessment much easier partly by reducing the time spent to collect the reference data through other mechanisms such as handheld GPS. Since the Landsat satellite images are well co-registered with Google earth images, collecting reference data for accuracy assessment purpose is more meaningful than collecting them through handheld GPS that could lead to an error up to 10 meters. However, caution should be taken while collecting reference data for accuracy assessment purpose. The coordinate of the point reference data

## 6. References

Blaschke T, Lang S (2006) Object based image analysis for automated information extraction—a synthesis. In: Measuring the Earth II ASPRS Fall Conference, San Antonio, TX: CD-ROM, pp: 6-10.

Blaschke T, Strobl J (2001) What's wrong with pixels? Some recent developments interfacing remote sensing and GIS. *GeoBIT/GIS* 6: 12-17.

Veljanovski T, Kanjir U, Ostir K (2011) Object-based image analysis of remote sensing data. *Geodetski vestnik* 55: 665-688.

Baatz M, Schäpe A (2000) Multi-resolution segmentation – an optimization approach for high quality multi-scale segmentation. In: Strobl J (ed.), *Angewandte Geographische Informationsverarbeitung XII*, Beiträge zum AGIT Symposium Salsburg 2000, Karlsruhe, Herbert Wichmann Verlag, Germany, pp: 12-23.

Willhauck G, Schneider T, De Kok R, Ammer U (2000) Comparison of object oriented classification techniques and standard image analysis for the use of change detection between SPOT multispectral satellite images and aerial photos.

should be placed well in the middle of a homogeneous land cover types, this should be made for three major reasons, a) to reduce location mismatch between reference points and the equivalent image objects on the classified image, b) Reference points are matched to segmented image objects on the classified map thus we have to be sure that similar cover type should exist up to a certain distance in all direction from the reference points, and c) the spatial resolution of the Google earth image is finer than that of the Landsat satellite images.

Proceedings of XIX ISPRS Congress 33: 35-42.

Hay GJ, Castilla G, Wulder MA, Ruiz JR (2005) An automated object-based approach for the multiscale image segmentation of forest scenes. *International Journal of Applied Earth Observation and Geoinformation* 7: 339-359.

Kamagata N, Akamatsu Y, Mori M, Qing Li Y, Hoshino Y, et al. (2005) Comparison of pixel-based and object-based classifications of high resolution satellite data in urban fringe areas. In: Proceedings of the 26th Asian Conference on Remote Sensing. Hanoi, Vietnam 7: 11.

Manakos I, Schneider T, Ammer U (2000) A comparison between the ISODATA and the eCognition classification methods on basis of field data. *IAPRS* 33: 133-139.

Whiteside T, Ahmad W (2005) A comparison of object-oriented and pixel-based classification methods for mapping land cover in northern Australia. In: Proceedings of SSC2005 Spatial intelligence, innovation and praxis: The National Biennial Conference of the Spatial Sciences Institute, pp: 1225-1231.

Yan G, Mas JF, Maathuis BHP, Xiangmin Z, Van Dijk PM (2006)

Comparison of pixel-based and object-oriented image classification approaches—a case study in a coal fire area, Wuda, Inner Mongolia, China. *International Journal of Remote Sensing* 27: 4039-4055.

Hay GJ, Castilla G (2006) Object-based image analysis: strengths, weaknesses, opportunities and threats (SWOT). In Proc. 1st Int Conf OBIA, pp: 4-5.

Benz UC, Hofmann P, Willhauck G, Lingenfelder I, Heynen M (2004) Multi-resolution, object-oriented fuzzy analysis of remote sensing data for GIS-ready information. *ISPRS Journal of photogrammetry and remote sensing* 58: 239-258.

Lavigne DA, Hong G, Zhang Y (2006) Performance assessment of automated feature extraction tools on high resolution imagery. In MAPPS/ASPRS Fall Conference 2006.

Blaschke T, Lang S, Hay G (2008) Object-based image analysis: spatial concepts for knowledge-driven remote sensing applications. Springer Science & Business Media, Berlin, Germany.

Schiwe J (2002) Segmentation of high-resolution remotely sensed data—concepts, applications and problems. *International Archives of Photogrammetry Remote Sensing and Spatial Information Sciences* 34: 380-385.

Nussbaum S, Menz G (2008) Object-based image analysis and treaty verification: new approaches in remote sensing—applied to nuclear facilities in Iran. Springer Science & Business Media, Berlin, Germany.

Haralick RM, Shapiro LG (1985) Image segmentation techniques. *Computer vision, graphics, and image processing* 29: 100-132.

Akjol D, Olaf H (2014) Extraction of built-up areas from Landsat imagery using the object-oriented classification method. AIS 2014, 9th International Symposium on Applied Informatics and Related Areas. Székesfehérvár, Hungary.

Zha Y, Gao J, Ni S (2003) Use of normalized difference built-up index in automatically mapping urban areas from TM imagery. *International Journal of Remote Sensing* 24: 583-594.

Xu H (2007) Extraction of urban built-up land features from Landsat imagery using a thematic-oriented index combination technique. *Photogrammetric Engineering & Remote Sensing* 73: 1381-1391.

Xu H (2008) A new index for delineating built-up land features in satellite imagery. *International Journal of Remote Sensing* 29: 4269-4276.

Sazzad TS, Islam S, Mamun MRK, Hasan MZ (2013) Establishment of an efficient color model from existing models for better gamma encoding in image processing. *International Journal of Image Processing* 7: 90.

Choodarathnakara AL, Kumar TA, Shivaprakash Koliwad DC (2012) Satellite Image Classification with Fuzzy Logic: from Hard to Soft Computing Situation. *International Journal of Computer Science & Applications*. Volume 1.

Navulur K (2007) Multi-spectral image analysis using the object oriented paradigm. CRC Press, Taylor & Francis Group, USA.

Thu TT, Lan PT, Ai TT (2013) Rule set of object-oriented classification using Landsat imagery in Donganh, Hanoi, Vietnam. *Journal of the Korean Society of Surveying, Geodesy, Photogrammetry and Cartography* 31: 521-527.

Nedeljkovic I (2004) Image classification based on fuzzy logic. *The International Archives of the Photogrammetry, Remote Sensing and Spatial Information Sciences* 34: 685.

Hofmann P, Lohmann P (2007) A strategy for quality assurance of land-cover/ land-use interpretation results with faulty or obsolete reference data. *The International Archives of the Photogrammetry, Remote Sensing and Spatial Information Sciences*.

Worako AW (2016) Land Use Land Cover Change Detection by Using Remote Sensing Data in Akaki River Basin. *International Journal of Environment, Agriculture and Biotechnology* 1: 1-10.

Kasa L, Zeleke G, Alemu D, Hagos F, Heinimann A (2011) Impact of Urbanization of Addis Ababa City on Peri-Urban Environment and Livelihoods.